Synthesis of Reactive Nano-Fe/Pd Bimetallic System-Impregnated Activated Carbon for the Simultaneous Adsorption and Dechlorination of PCBs

Hyeok Choi,[†] Souhail R. Al-Abed,*[,†] Shirish Agarwal,[‡] and Dionysios D. Dionysiou[‡]

National Risk Management Research Laboratory, U.S. Environmental Protection Agency, 26 W. Martin Luther King Drive, Cincinnati, Ohio 45268, and Department of Civil and Environmental Engineering, University of Cincinnati, Cincinnati, Ohio 45221-0071

Received February 4, 2008. Revised Manuscript Received March 17, 2008

Synthesis and use of reactive metal particles have shown significant environmental implications for the remediation of groundwater and sediment contaminated with chlorinated compounds. Herein, we have developed an effective strategy, employing a series of innovative granular activated carbon (GAC) composites incorporated with iron/palladium (Fe/Pd) bimetallic nanoparticles. The physical adsorption of polychlorinated biphenyls (PCBs) to GAC and their electrochemical dechlorination by Fe/Pd bimetal on the GAC could be simultaneously achieved. The novel synthesis approaches and targets to achieve in this study are (i) introduction of mesoporous GAC for Fe/Pd bimetal placement, (ii) in situ formation and incorporation of Fe particles in the GAC pores, (iii) modification of Fe surface with a discontinuous layer of noble metal Pd, and (iv) nanoscaling of Fe and Pd particles. Fe was imbedded in 7−40 nm mesoporous GAC via an incipient wetness impregnation method employing $Fe(NO_3)_3$. Heat-treated GAC/Fe (as Fe_2O_3) at 300 °C was reduced to GAC/zerovalent iron (ZVI) using $NaBH_4$ solution, and then Pd was reductively deposited to the ZVI surface from $Pd(CH_3CO_2)_2$. The resulting GAC/ZVI/Pd had high surface area of 358 m^2/g and pore volume of 0.352 cm^3/g for PCBs adsorption and 14.4% Fe and 0.68% Pd contents for PCBs dechlorination. The confinement of Fe crystal growth in the mesopores of GAC resulted in small 6−12 nm Fe nanoparticles on which 2−3 nm Pd nanoislands were well-distributed. Fe and Pd particles were mechanically stable (negligible leaching) due to a strong Fe−GAC metal−support interaction during calcination and Fe−Pd corrosion cell formation during Pd deposition. The GAC/ZVI/Pd system exhibited an efficient dechlorination of 2-chlorobiphenyl (2-ClBP) at 90% after 2 days and complete adsorption of 2-ClBP remaining, and the dechlorination product, biphenyl, formed.

Introduction

Recently, the synthesis and use of reactive zerovalent metals such as iron (Fe) and magnesium (Mg) have been documented to work efficiently for the dechlorination of chlorinated compounds such as carcinogenic polychlorinated biphenyls (PCBs) found in groundwater and sediment.[1–4]Two main strategies have been attempted to increase the reactivity of the metallic system. Since Fe or Mg is oxidized more rapidly when coupled with less active metals (Pd, Pt, Ni, Ag), deposition of such a noble metal to the Fe or Mg surface can significantly enhance the generation of electrons available for the dechlorination of PCBs.[5–7] Particularly for zerovalent iron/Pd (ZVI/Pd) systems, the kinetics of the dechlorination reaction can be further increased by introducing nanosize ZVI particles and Pd nanoislands.[1,2,7,8] The reactivity of ZVI is primarily controlled by the composition and availability of its near surface regime because the reductive dechlorination reaction initiated by ZVI is surface-mediated.[9] The small size and high surface to volume ratio of nanosize Fe (30−100 nm) make it attractive for the reaction, compared to those of conventional micrometer size Fe. The high reactivity of nanoscale ZVI/Pd system seems promising in case of liquid phase treatment, focusing on reaction mechanisms, contaminant degradation kinetics, and reaction products.

However, some scientific and technical challenges of the ZVI system below should be addressed for in situ remediation of contaminated sites with PCBs (or other hydrophobic compounds): (i) availability of PCBs for adsorption onto the surface of ZVI particles is very limited since they tend to strongly attach to organic substances in the environment (especially carbonaceous materials in soil) and they have extremely low solubility in water (at most, 4−5 mg/L),[10,11] (ii) control and maintenance of the dechlorination reaction by ZVI with high reactivity are required to respond to long-

* To whom correspondence should be addressed. E-mail: al-abed.souhail@epa.gov. Phone: +1 513-569-7849. Fax: +1 513-569-7879.
[†] U.S. Environmental Protection Agency.
[‡] University of Cincinnati.

(1) Zhang, W.-X. *J. Nanoparticle Res.* **2003**, *5*, 323.
(2) Wang, C. B.; Zhang, W. X. *Environ. Sci. Technol.* **1997**, *31*, 2154.
(3) Liu, Y.; Choi, H.; Dionysiou, D. D.; Lowry, G. V. *Chem. Mater.* **2005**, *17*, 5315.
(4) Fang, Y.; Al-Abed, S. R. *Environ. Sci. Technol.* **2007**, *41*, 6253.
(5) Grittini, C.; Malcomson, M.; Fernando, Q.; Korte, N. *Environ. Sci. Technol.* **1995**, *29*, 2898.
(6) Schrick, B.; Blough, J. L.; Jones, A. D.; Mallouk, T. E. *Chem. Mater.* **2002**, *14*, 5140.
(7) Agarwal, S.; Al-Abed, R. S.; Dionysiou, D. D. *Environ. Sci. Technol.* **2007**, *41*, 3722.
(8) Elliott, D. W.; Zhang, W.-X. *Environ. Sci. Technol.* **2001**, *35*, 4922.
(9) Gaspar, D. J.; Lea, A. S.; Engelhard, M. H.; Baer, D. R. *Langmuir* **2002**, *18*, 7688.

10.1021/cm8003613 CCC: $40.75
Published on Web 05/07/2008

term slow release of PCBs in sediment to aqueous phase, and (iii) injection and dispersion of colloidal and particulate ZVI are a critical hurdle when they are introduced to field application with the concept of a capping barrier where a physical layer of PCB-free clean sand is added to isolate the contaminated sites from the surrounding environment above the cap after placement.[12,13]

Herein, we have developed a new strategy, employing a series of adsorptive granular activated carbon (GAC) composites incorporated with reactive ZVI and Pd bimetallic nanoparticles (GAC/ZVI/Pd). The GAC/ZVI/Pd system can synergistically combine two strategies: (i) the use of GAC for physical adsorption of PCBs and (ii) the use of ZVI/Pd for the chemical dechlorination of PCBs. Due to their high adsorption capacity, carbon materials have been widely used as a support of Fe for various applications such as Fenton-like reaction[14] and Fischer−Tropsch synthesis.[15] Through a synthesis procedure that includes consecutive steps of an incipient wetness impregnation method, heat-treatment, borohydride reduction, and Pd doping, we attempted to tailor-design the physicochemical properties of GAC/ZVI/Pd for enhanced adsorption and dechlorination of PCBs. The specific synthesis approaches of this study are (i) introduction of mesoporous GAC as a support material for ZVI particles to disperse and as an adsorptive material for PCBs to contact with ZVI particles on the GAC, (ii) in situ formation and incorporation of Fe particles in the GAC pores to increase their mechanical stability, (iii) modification of Fe surface with a discontinuous layer of noble metal Pd to facilitate electron generation for PCBs dechlorination, and (iv) nanoscaling of ZVI and Pd particles via the restriction of Fe crystal growth in the GAC pores and reductive deposition of Pd to the ZVI to enhance their reactivity.

In this paper, we report, for the first time, the concept of the reactive GAC/ZVI/Pd system, novel preparation and characterization of a series of GAC/ZVI/Pd composites, and results on the adsorption and dechlorination of PCBs.

Experimental Section

Synthesis of Materials. Mesoporous GAC (HD 3000, Norit Americas Inc.) was washed with deionized water and dried at 110 °C overnight (A: GAC). Iron was incorporated into the GAC via an incipient wetness impregnation method, where 22.8 g of $Fe(NO_3)_3 \cdot 9H_2O$ (Fisher) was melted at 55−60 °C with a small quantity of water (5 mL) and then mixed with 10 g of GAC for 10 min. For total incorporation of Fe to the GAC, the slurry was dried at room temperature for 4 h followed by at 60−70 °C using an infrared ramp for 2 h (B: GAC/Fe_{salt}). The GAC/Fe_{salt} was further calcined in a furnace (Paragon HT-22-D, Thermcraft). The temperature was ramped at a rate of 180 °C/h to 150 °C to remove any solvent and moisture and held for 1 h. Then it was increased to 300 °C to remove nitrate ions, held for 4 h, and allowed to cool down naturally. Unincorporated free Fe was removed using a no. 20 sieve (USA Standard Testing Sieve) (C: GAC/Fe, here Fe is Fe_2O_3).

To reduce Fe(III) to elemental Fe, 1.6 g of $NaBH_4$ (Fisher) was prepared in 20 mL water. GAC/Fe of 4 g was resuspended in 50 mL of methanol/DI water (30/70, v/v). A 5 N NaOH solution was added to the GAC/Fe suspension drop by drop to bring the pH above 6.5. Then, $NaBH_4$ solution was added slowly to the pH-adjusted GAC/Fe suspension, and the mixture was stirred until no significant H_2 production was observed (∼3 h). This reduction procedure should be performed very carefully because of the production of explosive H_2. Then the GAC composite was recovered by filtering the slurry with a no. 20 sieve, washed with copious amounts of methanol to remove free ZVI and other impurities, and then dried at room temperature overnight (D: GAC/ZVI). For Pd doping, 75 mg of palladium acetate ($Pd(CH_3CO_2)_2$, Sigma) was dissolved in 20 mL of methanol for 2 h. Then GAC/ZVI was immersed into the Pd solution and stirred for 30 min. The other procedures for separation, washing, and drying were the same as for GAC/ZVI (E: GAC/ZVI/Pd). We will focus more on this sample E in comparison with A: GAC. The procedures for synthesis, storage, and handling of GAC/ZVI and GAC/ZVI/Pd samples were performed in an anaerobic chamber with condition of oxygen 0 ppm and hydrogen 3.5%. At the end of each procedure, samples were sieved with a no. 20 sieve to remove grains smaller than 0.85 mm.

Characterization. X-ray diffraction (XRD) analysis using a Kristalloflex D500 diffractometer (Siemens) with Cu Kα (λ = 1.5406 Å) radiation was employed to determine the crystal structure and crystallinity of GAC composites. A Tristar 3000 (Micromeritics) porosimetry analyzer was used to determine structural characteristics of GAC composites, including surface area (i.e., Brunauer, Emmett, and Teller (BET) surface area, Barrett, Joyner and Halenda (BJH) surface area, micropore surface area), porosity, and pore size and distribution, using nitrogen adsorption and desorption isotherms. H_2-temperature programmed reduction (H_2-TPR) technique was adopted on AutoChem 2910 TPD/TPR instrument (Micromeritics) to investigate changes in Fe species immobilized on GAC upon the variation of temperature under H_2 environment. The particle morphology and crystallographic properties of GAC composites were investigated at the nanolevel using a JEM-2010F (JEOL) high resolution-transmission electron microscope (HR-TEM). Selected area electron diffraction (SAED) pattern was also recorded to identify ordered or amorphous nature of the material. An environmental scanning electron microscope (ESEM, Philips XL 30 ESEM-FEG) was used to observe the surfaces of GAC composites at microlevel and to confirm the homogeneity of Fe particles on GAC. An elemental composition analysis of GAC composites, including X-ray mapping of C, Fe, O, and Pd, was performed using energy dispersive X-ray spectroscope (EDX, Oxford Isis) connected to the HR-TEM and ESEM. The Fe and Pd metal content of GAC composites was determined by inductively coupled plasma-atomic emission spectrometer (ICP-AES, IRIS Intrepid, Thermo Electron Corporation) after microwave-assisted digestion of samples (EPA method 3051).

Batch Reactions. Carcinogenic PCBs were widely used as an excellent insulator in electrical equipment and industrial processes

(10) Luthy, R. G.; Aiken, G. R.; Brusseau, M. L.; Cunningham, S. D.; Gschwend, P. M.; Pignatello, J. J.; Reinhard, M.; Traina, S. J.; Weber, W. J.; Westall, J. C. *Environ. Sci. Technol.* **1997**, *31*, 3341.
(11) Saleh, N.; Sirk, K.; Liu, Y.; Phenrat, T.; Dufour, B.; Matyjaszewski, K.; Tilton, R. T.; Lowry, G. V. *Environ. Eng. Sci.* **2007**, *24*, 45.
(12) Schrick, B.; Hydutsky, B. W.; Blough, J. L.; Mallouk, T. E. *Chem. Mater.* **2004**, *16*, 2187.
(13) Ponder, S. M.; Darab, J. G.; Bucher, J.; Caulder, D.; Craig, I.; Davis, L.; Edelstein, N.; Lukens, W.; Nitsche, H.; Rao, L.; Shuh, D. K.; Mallouk, T. E. *Chem. Mater.* **2001**, *13*, 479.
(14) Ramirez, J. H.; Maldonado-Hodar, F. J.; Perez-Cadenas, A. F.; Moreno-Castilla, C.; Costa, C. A.; Madeira, L. M. *Appl. Catal., B* **2007**, *75*, 312.
(15) Ma, W.; Kugler, E. L.; Dadyburjor, D. B. *Energy Fuels* **2007**, *21*, 1832.

until the mid-1970s.[16] Due to their persistent and hydrophobic nature, most of PCBs in the environment are found in soils and sediments, which act as a source for long-term release of PCBs to surface water and ecosystems. For the adsorption and dechlorination of 2-chlorobiphehyl (2-ClBP), one of the PCBs, 4 g of each GAC composite (GAC, GAC/Fe, GAC/ZVI, and GAC/ZVI/Pd) was added into 40 mL of 4 mg/L 2-ClBP (99%, Accustandard) aqueous solution (some were done with 1 g of GAC composite in 10 mL of solution for sacrificial batch). The solution was agitated using a gyroshaker at 60 rpm for 48 h. For each time interval, 0.5 mL of sample was taken using a gastight 1 mL glass syringe through septa cap, maintaining closed system conditions. 2-ClBP and the dechlorination product, biphenyl (BP) in aqueous phase, were extracted with 1 mL of hexane. Then, 0.5 mL of water-free supernatant organic phase was withdrawn, spiked with 10 μL of the internal standard (200 ppm D-8 naphthalene in dichloromethane), and analyzed in a gas chromatograph (GC, HP 6890)/mass spectrometer (MS, HP 5973) equipped with a SPB-5 column (Supelco). After 48 h of reaction, solid samples were also collected by centrifuging and removing supernatant. The collected samples were extracted in 20 mL of 50:50 acetone:hexane solution using a automated Soxhlet method to recover 2-ClBP and BP adsorbed on GAC composites. The other procedures were the same as for aqueous samples.

Results and Discussion

Synthesis Route. Microporous AC can provide a large number of sites for PCBs adsorption, but its small size pores limit ZVI immobilization on the grain boundary of AC (note Figure S1 and Table S1 in Supporting Information). Immobilization of ZVI/Pd in the porous structure of GAC is instrumental in improving its mechanical stability and increasing its dechlorination capability since adsorbed PCB molecules in the pores are also available for their dechlorination by the nearby ZVI/Pd. As shown in Figure S1, in addition to microporous structure which is useful for PCB adsorption, the HD3000 GAC used here shows type IV N_2 adsorption/desorption isotherms typical for well-developed mesoporous structure. The mesopore region in 10−40 nm might be a good candidate for ZVI/Pd placement. The GAC has high BET surface area of 574 m^2/g and large pore volume of 0.639 cm^3/g. Its BJH surface area (447 m^2/g) and pore volume (0.592 cm^3/g), which are calculated based on the mesoporous structure of a material, are significantly higher than those of the microporous GAC.

Scheme 1 shows the synthesis route of GAC/ZVI/Pd composites. To control the physicochemical properties of GAC composites at the nanolevel, Fe was in situ imbedded in the HD3000 mesoporous GAC via an incipient wetness impregnation method employing $Fe(NO_3)_3$. Among the Fe salts tested (ferric nitrate, ferric chloride, ferrous sulfate) as a starting material for ZVI, ferric nitrate was chosen because other counterpart anions (Cl^- and SO_4^{2-}) could not be completely removed during the heat-treatment procedure at 300 °C, which might affect Fe-GAC metal−support interaction during calcination followed by Fe reduction.[17] Mixing A: GAC with ferric nitrate resulted in gel-like solid matrix at pH 3−4. During calcination of B: GAC/Fe(III) at 300 °C, all nitrate ions were removed and iron ions transformed into iron oxides (C: GAC/Fe). It is notable that the crystal growth of iron oxides should be restricted within the GAC pores in mainly the meso- (1.7−50 nm) and partially micro- (less than 1.7 nm) ranges.[18] The heat-treatment procedure was critical to increase mechanical stability of Fe and thus keep Fe firmly attached to GAC in the subsequent steps. In case of the absence of the calcination procedure, no significant amounts of Fe and Pd were present in the resulting GAC/ZVI/Pd, and thus negligible 2-ClBP dechlorination was observed. During the reaction of GAC/Fe with $NaBH_4$, the iron oxides were reduced to elemental Fe (D: GAC/ZVI).[19]

$$4Fe^{3+} + 3BH_4^- + 9H_2O \rightarrow 4Fe^0 + 3H_2BO_3^- + 12H^+ + 6H_2 \quad (1)$$

Before the reduction of GAC/Fe, pH adjustment of GAC/Fe to above 6.5 was needed since the acidic pH of GAC/Fe is adverse for the reduction of Fe. Then the GAC/ZVI was doped with Pd, which was reductively deposited from $Pd(CH_3CO_2)_2$ as elemental Pd islands on the ZVI surface (E: GAC/ZVI/Pd).

$$Fe^0 + Pd^2 \rightarrow Fe^2 + Pd_0\downarrow \quad (2)$$

The Fe/Pd system is known to create numerous isolated galvanic cells where bulk Fe particles as an anode are

Scheme 1. Synthesis Route of GAC/ZVI/Pd Composites[a]

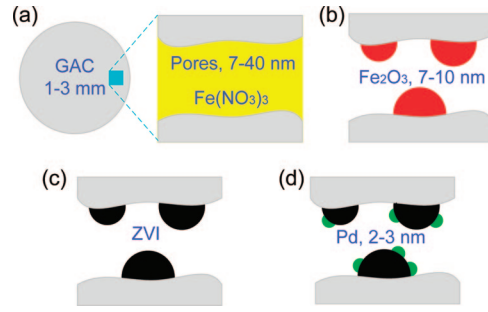

[a] (a) Embedding of mesoporous GAC with $Fe(NO_3)_3$ salt via incipient wetness impregnation method, (b) formation of nanosize iron oxide crystal, Fe_2O_3, in the pores of GAC during calcination, (c) reduction of Fe_2O_3 to elemental Fe using $NaBH_4$ solution, and (d) reductive deposition of Pd to Fe surface from Pd $(CH_3CO_2)_2$.

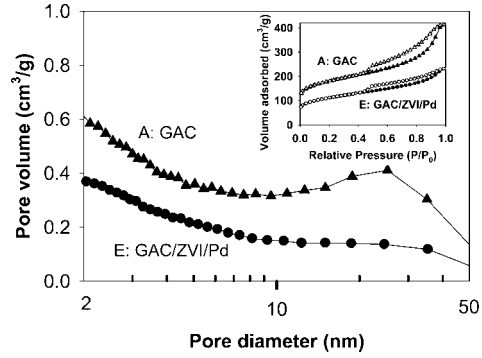

Figure 1. BJH adsorption pore size distribution of GAC composites. Inset is their N_2 adsorption/desorption isotherms.

(16) Ross, G. *Ecotoxicol. Environ. Saf.* **2004**, *59*, 275.

(17) Yang, Q.; Choi, H.; Chen, Y.; Dionysiou, D. D. *Appl. Catal., B* **2008**, *77*, 300.

(18) Martin-Martinez, J. M.; Vanice, M. A. *Ind. Eng. Chem. Res.* **1991**, *30*, 2263.

Table 1. Structural and Crystallographic Properties and Metal Content of GAC Composites

		surface area (m^2/g)			pore volume (cm^3/g)			pore size (nm)		content[e] (%)		crystal phase and size[f] (nm)	
entry	composition	BET	micro[a]	BJH[b]	total[c]	micro[a]	BJH[b]	ave[d]	BJH[b]	Fe	Pd	Fe	Pd
A	GAC	574	226	447	0.639	0.124	0.592	4.45	5.30	<0.01			
B	GAC/Fe_{salt}	366	158	326	0.382	0.087	0.369	4.18	4.54	11.4		disordered	
C	GAC/Fe	468	116	360	0.489	0.064	0.432	4.18	4.79	11.8		Fe_2O_3, 7−10	
D	GAC/ZVI	369	102	269	0.375	0.056	0.327	4.07	4.85	9.5		Fe^0+Fe_2O_3, 7−11	
E	GAC/ZVI/Pd	358	98.0	260	0.352	0.054	0.302	3.94	4.66	14.4	0.68	Fe^0+Fe_2O_3, 9−12	Pd^0, 2−3

[a] Micro: *t*-plot micropore. [b] BJH: cumulative pores between 1.7 and 300 nm from BJH adsorption branch. [c] Single point adsorption total pore volume at $P/P_0 = 0.99$ (corresponding to less than 200 nm pores). [d] Adsorption average pore width (4 V/A by BET). [e] Based on ICP-AES analysis. [f] Based on HR-TEM observation and XRD measurement.

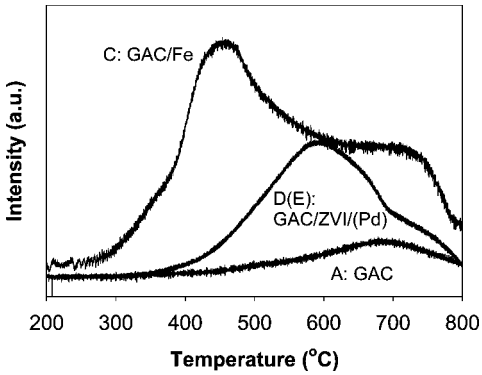

Figure 2. H_2-TPR patterns of GAC composites. TPR pattern of GAC/ZVI/Pd is almost identical to that of GAC/ZVI.

preferably oxidized while Pd islands as a cathode are protected and remain uncharged.[5,7]

Physical Structure. As shown in Figure 1, the mesoporous structure of GAC, especially in the range of 7−40 nm, was well occupied by ZVI/Pd particles. A small hysteresis loop between adsorption and desorption isotherms of GAC/ZVI/Pd implies that the route to inner tiny pores was partially blocked by ZVI/Pd particles (note Figure S2 in Supporting Information for the porosimetry results of all GAC composites). The changes in the physicochemical properties of GAC composites during their synthesis demonstrated in Table 1 reflect the synthesis route and chemistry. The BET surface area (i) decreased from 574 m^2/g to 366 m^2/g due to impregnation of $Fe(NO_3)_3$, (ii) increased to 468 m^2/g due to thermal decomposition of NO_3^- and crystallization (compactness) of Fe to iron oxide, and (iii) decreased to 369 m^2/g due to reduction of Fe_2O_3 to disordered Fe^0 and possibly formation of boron shell around the Fe^0 core.[3] Finally, around 38% of BET surface area and 45% of pore volume of GAC were occupied by Fe/Pd particles with PCBs dechlorination function. The ZVI/Pd-impregnated GAC still had high surface area of 358 m^2/g and pore volume of 0.352 cm^3/g, which act as adsorptive sites for PCBs (it is important to control the ratio of impregnated ZVI/Pd content to remaining GAC pores). The pore sizes of GAC composites were smaller than those of neat GAC due to the pore blocking and impregnation of Fe/Pd.

Fe Species, Metal Content, Crystal Phase, and Size. TPR is a useful tool to differentiate various iron species in GAC composites as well as to obtain insights on metal−support interactions. Figure 2 shows the H_2-TPR patterns of GAC/Fe composites (also note Figure S3, Supporting Information). For GAC/Fe (as Fe_2O_3), the first major peak centered at 450 °C corresponds to the reduction of Fe_2O_3 to Fe_3O_4 ($3Fe_2O_3 + H_2 \rightarrow 2Fe_3O_4 + H_2O$) which is further reduced to Fe^0 ($Fe_3O_4 + 4H_2 \rightarrow 3Fe^0 + 4H_2O$).[20] The second broad minor peak centered at 700 °C could be assigned to two transformations: One below 700 °C explains the reduction of Fe_3O_4 to FeO ($Fe_3O_4 + H_2 \rightarrow 3FeO + H_2O$) and another above 700 °C corresponds to the reduction of FeO to Fe^0 ($FeO + H_2 \rightarrow Fe^0 + H_2O$). Reduction of unsupported Fe_2O_3 to Fe^0 typically occurs at around 350−400 °C.[20,21] The higher reduction temperature (450 °C) of Fe_2O_3 incorporated with GAC implies that a strong Fe-GAC metal−support interaction apparently exists.[21] The interaction might be partly because of the high dispersion of Fe in the porous structure of GAC, which can suppress the formation of large size crystals of Fe_2O_3. The TPR pattern of D: GAC/ZVI is intriguing since iron species in the composite would be mainly Fe^0 and Fe_2O_3 and partially Fe_3O_4 and FeO. One wide peak centered at 580 °C indicates the presence of reduced forms of Fe in the D sample rather than Fe_2O_3. However, the peak also implies that some of Fe_2O_3 most probably in tiny GAC pores was not reduced to Fe^0 effectively, and the intimate contact between Fe and GAC during calcination might lead to the formation of hard-to-reduce iron−GAC composites as well as iron carbides.[22,23] The TPR pattern of GAC/ZVI/Pd was almost the same as that of GAC/ZVI.

Table 1 summarizes the contents of Fe and Pd in GAC composites and their crystallographic properties (note Figure S4, Supporting Information, for the XRD patterns of all GAC composites). Fe content was very stable at around 11−14%. Pd loading was 0.68%. Fe-based Pd content was 4.7% which is much higher than the optimum Pd content in Fe/Pd system reported elsewhere since Pd islands here are also present on GAC directly.[5,24] Fe in C: GAC/Fe was identified as Fe_2O_3. The size of Fe immobilized in the GAC pores was 7−12 nm smaller than a typical size of nano ZVI.[2,3] This strongly suggests that the GAC pores acted as a template for Fe particle growth. A previous study showed the porous structure of carbon greatly influenced Fe crystallite size and particle size distribution.[18] The size of Pd was confined at 2−3 nm.

(19) Liu, Y.; Majetich, S. A.; Tilton, R. D.; Sholl, D. S.; Lowry, G. V. *Environ. Sci. Technol.* **2005**, *39*, 1338.
(20) Mauvezin, M.; Delahay, G.; Coq, B.; Kieger, S.; Jumas, J. C.; Olivier-Fourcade, J. *J. Phys. Chem. B* **2001**, *105*, 928.
(21) Zhang, C.-H.; Wan, H.-J.; Yang, Y.; Xiang, H.-W.; Li, Y.-W. *Catal. Commun.* **2006**, *7*, 733.
(22) Ma, W.; Kugler, E. L.; Wright, J.; Dadyburjor, D. B. *Energy Fuels* **2006**, *20*, 2299.
(23) Schwickardi, M.; Olejnik, S.; Salabas, E.-L.; Schmidt, W.; Schüth, F. *Chem. Commun.* **2006**, 3987.
(24) Morales, J.; Hutcheson, R.; Cheng, F. *J. Hazard. Mater.* **2002**, *90*, 97.

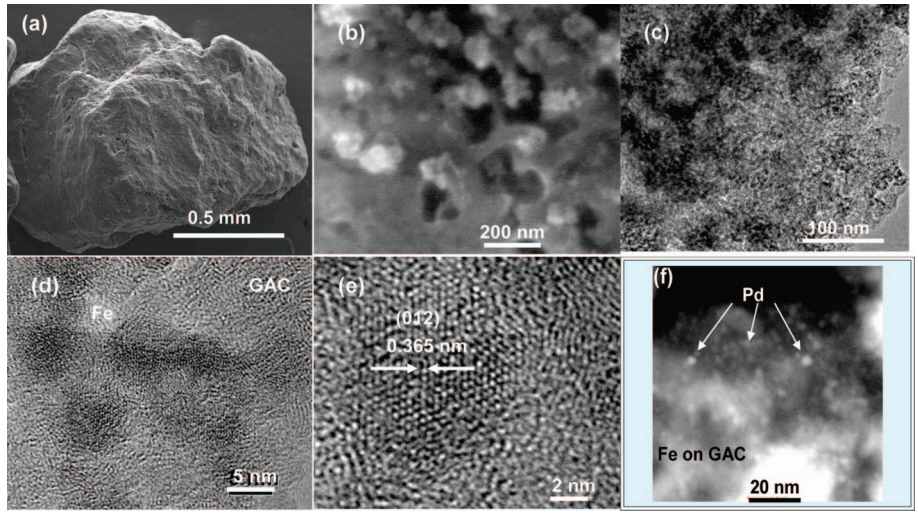

Figure 3. Micro- and nanoscale visual morphology of GAC/ZVI/Pd composite. (a) ESEM image of GAC/ZVI/Pd grain, (b) ESEM image of the cross-section of GAC/ZVI/Pd, suggesting that many macro- and mesopores of GAC are occupied by Fe/Pd particles, (c) HR-TEM image of GAC/ZVI/Pd composite, showing Fe/Pd-embedded GAC matrix, (d and e) HR-TEM image of Fe nanoparticles impregnated on GAC, showing obvious lattice fringes of Fe_2O_3, and (f) scanning-TEM image of Pd nanoislands on the surface of GAC/Fe, based on Z-contrast image (i.e., the contrast originates from the elemental difference).

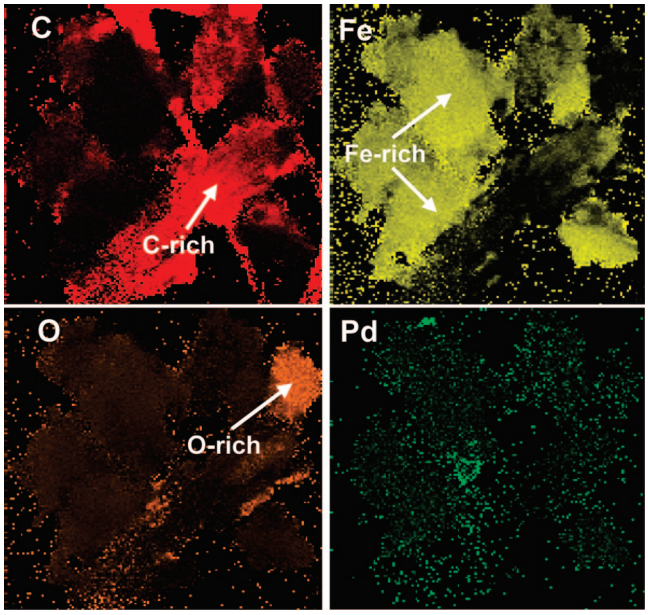

Figure 4. X-ray mapping of Fe-rich phase (2 μm × 2 μm area) in GAC/ZVI/Pd for C, Fe, O, and Pd elements. The GAC as a background material is covered by Fe but some regions are C-rich phase. Most of Fe species are identified as ZVI.

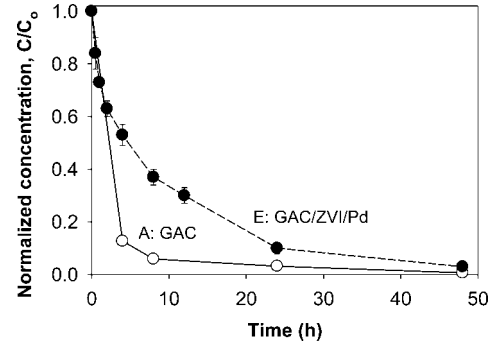

Figure 5. Disappearance kinetics of 2-ClBP in liquid phase with GAC and GAC/ZVI/Pd, resulting from adsorption and/or dechlorination of 2-ClBP. Error bars indicate the standard deviation of triplicated results on 2 days of reaction of 4 mg/L 2-ClBP solution with 100 g/L AC materials.

Morphology and Elemental Composition. The visual structure and bonding morphology of GAC composites at micro- and nanoscale are presented in Figure 3 (also note Figure S5, Supporting Information). Figure 3a shows ~1.5 mm GAC grain incorporated with ZVI/Pd bimetallic particles. The cross section of GAC/ZVI/Pd in Figure 3b suggests that the macro- and mesopores of GAC are well occupied by agglomerated ZVI/Pd particles. Neat GAC has a distinct microporous structure, originated from disordered graphitic layers and primary nanosize particles showing concentric arrangements of stacked graphitic layers (Figure S5a,b), while it has also well-defined 5−10 nm interconnected mesoporous structure (Figure S5c). In Figure 3c, the low contrast area (or dark spots) indicates ZVI/Pd nanoparticles-rich phase, suggesting that many of the micropores and mesopores disappeared. As shown in Figure 3d, 7−8 nm well defined Fe nanoparticles are impregnated on GAC. Due to their distinct crystal lattice fringes, Fe particles are easily differentiated from the highly disordered (amorphous) phase of GAC material as a background. As the strong metal−support interaction was observed in TPR analysis, the Fe particles are shown to be completely impregnated into GAC matrix (i.e., conjunction of the lattice planes of Fe particles with the graphitic sheets in the surrounding carbon shells) rather than just sitting on GAC. D spaces of 3.65, 2.73, and 2.48 Å observed in Figure 3e matched with the theoretical values of Fe_2O_3 (rhombohedral, 2000 JCPDS 87-1164) at Miller indices of (012), (104), and (110), respectively. Figure 3f shows scanning-TEM image of Pd nanoislands on the surface of GAC/Fe. The image was based on Z-contrast. Elements, like Pd, with higher atomic number appear brighter relative to low Z elements, such as Fe and C. Bright spots indicate Pd particles. Distinct 2−3 nm Pd particles are well distributed on GAC/Fe matrix. The presence of ordered crystal phases including Fe_2O_3 was confirmed using selected area electron diffraction patterns (Figures S5e). Figure 4 shows a two-dimensional X-ray mapping of Fe-rich phase (2 μm × 2 μm area) to investigate the distribution of C, Fe, O, and Pd

Table 2. Partitioning of 2-ClBP Remaining and BP Formed between Aqueous and Solid Phases, 2-ClBP and BP Extraction Efficiency from Solid Phase, and 2-ClBP Dechlorination Efficiency of GAC Composites[a]

		liquid phase		adsorption[b]	extracted solid phase[c]		solid extraction[d]	recovery[e]			
entry	composition	2-ClBP	BP	overall	2-ClBP	BP	Overall	2-ClBP	BP	overall	dechlorination[f]
A	GAC	0.17	0.32	99.5	91.1	0.30	91.9	91.3	0.62	91.9	
C	GAC/Fe	1.50	0.30	98.2	80.2	0.73	82.4	81.7	1.03	82.7	
D	GAC/ZVI	0.70	0.30	99.0	82.0	0.67	83.5	82.7	0.97	83.7	1.16
E	GAC/ZVI/Pd	0.54	0.30	99.2	2.48	26.7	29.4[h]	3.02	27.0	30.0[h]	90.0
(E)[g]		(3.47)	(0.55)	(96.0)	(0.78)	(5.28)	(6.31)	(4.25)	(5.83)	(10.08)	(57.8)

[a] % after 2 days reaction of 4 mg/L 2-ClBP solution with 100 g/L GAC composite. [b] Corresponds to overall solid phase. [c] Extracted 2-ClBP and BP in solid phase using Soxhlet. [d] Solid extraction efficiency = extracted solid phase/solid phase × 100. [e] Recovery from liquid and solid phase. [f] Dechlorination efficiency, based on BP recovery/overall recovery × 100. [g] GAC/ZVI/Pd prepared without pH adjustment to 6.5. [h] Low recovery (extraction) in case of GAC/ZVI/Pd is due to BP, which is believed to be strongly adsorbed to GAC/ZVI/Pd.

elements in the GAC matrix. The GAC as a background material is covered by Fe, but some regions are in the C-rich phase. Most of Fe species are identified as ZVI since the O signal in the Fe-rich phase is very weak. Some O-rich areas (e.g., right top area highlighted with an arrow) were found. This implies the presence of Fe_2O_3, which was not transformed to Fe^0 accordingly during its reduction, because such an O-rich phase was not observed in neat GAC where weak O signal from oxidized carbon functional groups was relatively well distributed to the whole area. This is in good agreement with the TPR observation. Pd was uniformly deposited to GAC/ZVI surface.

PCBs Adsorption and Dechlorination. The simultaneous adsorption and dechlorination of 2-ClBP was tested using the GAC composites. Figure 5 shows the kinetics of disappearance of 2-ClBP in the aqueous phase. Adsorption of 2-ClBP to neat GAC with the highest surface area was very fast while GAC/ZVI/Pd exhibited a pseudofirst order reaction for 2-ClBP removal, resulting from the combination of adsorption and dechlorination. Table 2 summarizes partitioning of 2-ClBP remaining and BP formed between aqueous and solid phases and 2-ClBP dechlorination efficiency after 48 h reaction. All GAC composites showed almost complete 2-ClBP removal from the liquid phase above 98−99%. It is notable that in the case of GAC/ZVI/Pd, only 0.3% of BP was partitioned into the liquid phase. This strongly suggests that even the BP, generated from the dechlorination of 2-ClBP by ZVI/Pd bimetal in GAC pores (eqs 3 and 4), is preferentially adsorbed to GAC rather than being diffused to the liquid phase. This can explain in part why the GAC/ZVI/Pd system has lower carbon recovery than other systems with no dechlorination reaction. The product BP is now available for their further decomposition and eventually mineralization by natural biological systems.

$$Fe^0 \rightarrow Fe^{2+}(aq) + 2e^-, \quad E_H{}^0 = +0.447\ V \tag{3}$$

$$Ar_2Cl + xH^+ + ye^- \rightarrow Ar_2(y-x) + (y-x)Cl^- \tag{4}$$

The GAC/ZVI/Pd dechlorinated 2-ClBP efficiently at 90% within 2 days compared to the negligible efficiency of GAC/ZVI since Pd doping to ZVI surface greatly affected the overall reaction through the facilitated oxidation of ZVI by less active Pd and Pd-meditated hydrogenation.[5,7,8] H_2, which is formed via a competing reaction of the released electrons with water (electrolysis of water) (eq 5), can be used to dechlorinate PCB via hydrodechlorination (eq 6). The dissociative activation of H_2(g) by Pd and Pd-catalyzed hydrodechlorination of PCBs by H_2(aq) have been reported (eq 7).[25,26] As mentioned in the synthesis route, the GAC/ZVI/Pd exhibited 56% higher dechlorination ability than that prepared without the pH adjustment during reduction of Fe_2O_3 to ZVI.

$$2H_2O + 2e^- \rightarrow H_2 + 2OH(aq)^-, \quad E_H{}^0 = -0.379\ V \tag{5}$$

$$H_2(g) \leftrightarrow 2H_{ad} \leftrightarrow 2H(aq)^+ + 2e^-, \quad E_H{}^0 = +0.379\ V \tag{6}$$

$$PdH_2 + Ar_2Cl \rightarrow Ar_2H + PdClH \tag{7}$$

The new reactive system employing the GAC/ZVI/Pd composite is hybrid and exhibits interesting properties, involving the following: (1) 2-ClBP is partitioned between liquid phase and GAC solid phase, (2) 2-ClBP contacted with ZVI/Pd on GAC is dechlorinated, forming an intermediate BP, and (3) the BP formed is rapidly adsorbed to GAC composite (dominantly) or diffused to liquid phase (negligibly).

Conclusions

For their synergistic and simultaneous function of adsorption and dechlorination of PCBs, reactive ZVI/Pd bimetallic nanoparticles were incorporated in the mesopores of GAC. The GAC/ZVI/Pd had a high surface area and pore volume available for PCBs adsorption and Fe and Pd contents available for PCBs dechlorination. The crystal growth of Fe was confined in the mesopores of GAC, and Pd was reductively deposited as elemental Pd islands onto the Fe surface, resulting in nanoscaling of Fe at 6−12 nm and Pd at 2−3 nm, respectively. Neat GAC and GAC/Fe exhibited only adsorption of 2-ClBP while GAC/ZVI/Pd showed a significant dechlorination of 2-ClBP and complete adsorption of the remaining 2-ClBP, and the reaction product BP formed. The hybrid GAC/ZVI/Pd system can be used for the fabrication of an efficient "reactive capping barrier" to in situ treat sediment and groundwater contaminated with hydrophobic organic compounds via reductive pathways.

Acknowledgment. This research was funded and conducted by the National Risk Management Research Laboratory of U.S. EPA, Cincinnati, Ohio. This paper has not been subjected to internal policy review of the U.S. Environmental Protection Agency. Therefore, the research results do not necessarily reflect

(25) Mitsui, T.; Ross, M. K.; Formin, E.; Ogletree, D. F.; Salmeron, M. *Nature* **2003**, *422*, 705.

the views of the agency or its policy. Mention of trade names and commercial products does not constitute endorsement or recommendation for use. The authors greatly appreciate Norit Americas Inc. for their generous donation of the activated carbon. The authors acknowledge the use of instruments purchased through the National Science Foundation CAREER award (BES, No. 0448117) for D.D.D.

Supporting Information Available: Porosimetry (Figures S1−S2 and Table S1), TPR (Figure S3), XRD (Figure S4), and ESEM and TEM (Figure S5) (PDF). This material is available free of charge via the Internet at http: //pubs.acs.org.

CM8003613

(26) Lowry, G. V.; Reinhard, M. *Environ. Sci. Technol.* **1999**, *33*, 1905.